George Bertsch - Lecture I

Computational Aspects

1. representations
2. exchange interaction
3. frequency-space methods
   scaling
4. direct time integration methods
5. Effect of zero-point nuclear motion on the response

} Lecture II

General Remarks

1. Terminology: Formalism, theory, method, algorithm

2. Measuring computational costs

   FPO $\approx C M N^{\alpha}$

3. Direct matrix algorithms N^3

4. Iterative algorithms for large matrices

   $N^2 M_{iter}$

   a) Krylov space: $\{x, Ax, A^2x, \ldots\}$

      i) diagonalization $Av = \lambda x$ Lanczos

      ii) $Av = b$ Conjugate Gradient

      only need to store 3 vectors

   b) Davidson space: $\left\{x, \frac{1}{D}Ax, \left(\frac{1}{D}A\right)^2 x, \ldots\right\}$

Some definitions:

formalism	operators, conditionally convergent integrals, ...
theory	functions,well-defined integrals and well-behaved DE's
method	representations, tranucated integrals and series
algorithm	computational procedure for a well-defined mathematical task
formula	equation whose right hand side has nothing more complicated than integrals over given functions

Direct matrix operations

$N \times N$ matrix

Operation	No. of floating point operations
multiplication AB	$2N^3$
inversion Gauss-Jordan	N^3
diagonalization Householder/ TQLI	$3N^3$
Fast Fourier Transform $Fv = \tilde{v}$	$5 N \log N$

Time-dependent density functional theory

Variational principle (Dirac?)

$$\delta \int dt \left(E[\varphi] - \sum_n \varphi_n^* \frac{i\partial}{\partial t} \varphi_n \right) = 0$$

↓

time-dependent Kohn-Sham equations

$$-\frac{\hbar^2}{2m}\nabla^2\varphi_n + \left(V_{ext}(t) + \frac{\delta V}{\delta n(r)} \right)\varphi_n = i\hbar\frac{\partial}{\partial t}\varphi_n$$

- satisfies conservation laws
- equivalent to RPA in small amplitude limit

Ways to solve equations:

1) linearize and make Fourier decomposition $t \to \omega$.

   a) diagonalize matrix equations (RPA) $Mx = \omega x$

   b) invert inhomogeneous matrix equation (linear response) $Mx = a$

2) solve in real-time $\varphi_n(t) = e^{-i\int H(t)dt}\varphi_n(0)$

Basic operation:

$$H_{KS}\,\phi_i$$

Representations:

a) plane wave (cond. mat.)

complex :: phi(N_orb : N_k)

$\langle \phi_i | k_m \rangle \quad 1 \le i \le N_{orb},\ 1 \le m \le N_k$

b) spatial mesh

$\langle \phi_i | r_m \rangle$ real for static KS

complex for time-dependent

c) atomic orbital basis (quantum chemistry)

Remarks:

1) plane waves are used in supercells.
2) PW and SM are essentially convertable by the FFT

$$\#\mathrm{FFT} \cong 5 N_k \log_2 N_k$$

3) PW and SM require pseudopotentials.
4) AO basis is not well suited for loosely bound electrons and for currents.
5) Accuracy of PW and SM is easily checked by changing momentum cutoff or mesh size.
6) H_{KS} is a sparse matrix in the SM representation provided V_{xc} is local or nearly local.

$H_{KS}\phi_j$ in the real-space method

```
SUBROUTINE hpsi(a_in,a_out)
implicit none

integer :: ix,iy,iz,i,j,a,lm,ik
real(8) :: wk(-Nx:Nx,-Nx:Nx,-Nx:Nx)

wk=0.d0

do i=1,ML ; wk(Lx(i),Ly(i),Lz(i))=a_in(i) ; end do

a_out(1:ML) = ( Vpsl(1:ML) + Vh(1:ML) + Vxc(1:ML) )*a_in(1:ML)

do i=1,ML
   ix=Lx(i) ; iy=Ly(i) ; iz=Lz(i)
   a_out(i)=a_out(i)+(-H2M)/H**2*(
&         +3*cN0*wk(ix,iy,iz)
&         +cN1*(wk(ix+1,iy,iz)+wk(ix-1,iy,iz)+wk(ix,iy+1,iz)
&              +wk(ix,iy-1,iz)+wk(ix,iy,iz+1)+wk(ix,iy,iz-1))
&         +cN2*(wk(ix+2,iy,iz)+wk(ix-2,iy,iz)+wk(ix,iy+2,iz)
&              +wk(ix,iy-2,iz)+wk(ix,iy,iz+2)+wk(ix,iy,iz-2))
&         +cN3*(wk(ix+3,iy,iz)+wk(ix-3,iy,iz)+wk(ix,iy+3,iz)
&              +wk(ix,iy-3,iz)+wk(ix,iy,iz+3)+wk(ix,iy,iz-3))
&         +cN4*(wk(ix+4,iy,iz)+wk(ix-4,iy,iz)+wk(ix,iy+4,iz)
&              +wk(ix,iy-4,iz)+wk(ix,iy,iz+4)+wk(ix,iy,iz-4)))
end do

return

END SUBROUTINE hpsi
```

Exchange Interaction: Computational Cost

LDA in spatial mesh basis:

$$V_{xc}\,\phi_j\big|_r = V_{xc}(r)\,\phi_j(r) \qquad N_{orb}\,N_r$$

any localized orbital basis has same scaling

Exact

$$V_{xc}\,\phi\big|_{j,r} = -\sum_{j'}\int d^3r'\,\frac{e^2}{|r-r'|}\,\phi_{j'}(r')\,\phi_{j'}(r)\,\phi_j(r')$$

$$N_{orb}\,N_r \qquad N_{orb}\,N_r \qquad \rightarrow \quad N_{orb}^2\,N_r^2$$

This can be sped up by a factor N_r by using an efficient Poisson solver to calculate

$$V_{j,j'}(r') = -\int d^3r'\,\frac{e^2}{|r-r'|}\,\phi_{j'}(r')\,\phi_j(r')$$

Other approach to speed up compatation:

$\frac{e^2}{|r-r'|}\sum_{j'}\phi_{j'}(r)\,\phi_{j'}(r')$ is small for $|r-r'|$ large.

therefore $\int d^3r' \sim M$ instead of N.

The real-time method for TDDFT

Equation to solve: $H_{KS}\,\phi_j = i\frac{\partial}{\partial t}\phi_j$

Initial condition

$$\phi_j(t=0) = e^{ikz}\phi_j^0 \qquad k \text{ "small"}$$

Time-dependent dipole moment

$$p_{zz}(t) = e^2 \int d^3r\; z \sum_j |\phi_j|^2$$

Dynamic polarizability

$$\alpha_{zz}(\omega) = \frac{1}{k}\int_0^\infty e^{-i\omega t}\, p_{zz}(t)\, dt$$

Thus a single calculation does all frequencies together. This trick is well-known in other fields, eg. FT-ICRMS.

Numerical methods for the time integrator

$$e^{-i H_{KS}\Delta t}\,\phi_j(t) = \phi_j(t+\Delta t).$$

1. Leap-frog
2. Flocard-Koonin-Weiss
3. Crank-Nicholson
4. Split Operator

Comparison of Methods

	FPO	Memory
ph matrix a) diagonalization	$(N_p N_{orb})^2 N_r$	$(N_p N_{orb})^2$
k-space response	$5 M_\omega N_k^3$	N_k^3
Response in r-space (Sternheimer)	$M_\omega M_{it} N_{orb} N_r$	$(N_{orb} + N_p) N_r$
Real Time	$N_{orb} N_r M_T$	$N_r N_{orb}$

M_T = number of time steps

a) often $(N_p N_{orb})$ can be severely truncated.

Fourier Transform Ion Cyclotron Resonance Mass Spectrometry

Alan G. Marshall

Center for Interdisciplinary Magnetic Resonance, National High Magnetic Field Laboratory, Florida State University, 1800 East Paul Dirac Drive, Tallahassee, FL 32310

As for Fourier transform infrared (FT-IR) interferometry and nuclear magnetic resonance (NMR) spectroscopy, the introduction of pulsed Fourier transform techinques revolutionized ion cyclotron resonance mass spectrometry: increased speed (factor of 10,000), increased sensitivity (factor of 100), increased mass resolution (factor of 10,000—an improvement *not* shared by the introduction of FT techniques to IR or NMR spectroscopy), increased mass range (factor of 500), and automated operation. FT-ICR mass spectrometry is the most versatile technique for unscrambling and quantifying ion-molecule reaction kinetics and equilibria in the absence of solvent (i.e., the gas phase). In addition, FT-ICR MS has the following *analytically* important features: speed (~1 second per spectrum); ultrahigh mass resolution *and* ultrahigh mass accuracy for analysis of mixtures and polymers; attomole sensitivity; MS^n with one spectrometer, including two-dimensional FT/FT-ICR/MS; positive and/or negative ions; multiple ion sources (especially MALDI and electrospray); biomolecular molecular weight and sequencing; LC/MS; and single-molecule detection up to 10^8 Dalton. Here, some basic features and recent developments of FT-ICR mass spectrometry are reviewed, with applications ranging from crude oil to molecular biology.

INTRODUCTION

Various aspects of the Fourier transform relationship between an interferogram and a spectrum were known to Michelson and Rayleigh, among others. Modern FT optical interferometry may be said to have originated from P. Fellgett's 1951 thesis at Cambridge University (1), and practical implementation of FT-IR spectroscopy exploded almost immediately following the introduction of the Cooley-Tukey fast Fourier transform algorithm (2), which has become the most highly cited paper in all of mathematics. FT-NMR was introduced in 1966 by Ernst and Anderson (3). However, it was another nine years before Fourier transform methods could be implemented in ion cyclotron resonance (4, 5). FT-ICR MS evolution since then has paralleled that of FT-NMR (6), much as FT-NMR borrowed many concepts from FT-interferometry. The growth of FT-ICR MS is graphically evident from Figure 1.

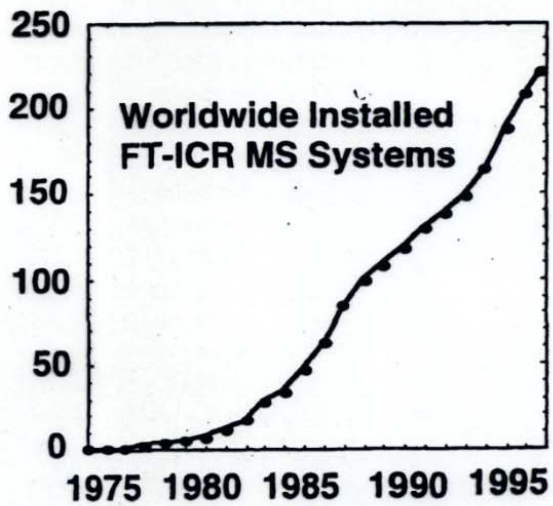

FIGURE 1. Following Comisarow/Marshall's first homebuilt instrument in December, 1973, the first commercial instrument (based on their 1976 patent) appeared in 1980.

CP430, *Fourier Transform Spectroscopy:* 11th International Conference
edited by J.A. de Haseth

More on time integrators

1. Leap-frog algorithm can be derived from a numerical Lagrangian; therefore satisfying norm and energy conservation.

variables: $\{\phi_{imt}\}$

i wave function component
m orbit
t discrete time index

$$\mathcal{L}(t) = \mathcal{E}(\{\phi_{imt}\}) - i\sum_{im}\phi^*_{imt}\left(\frac{\phi_{imt+\Delta t} - \phi_{imt-\Delta t}}{2\Delta t}\right)$$

$$\frac{\delta\mathcal{L}}{\delta\phi^*_{imt}} = \frac{\delta\mathcal{E}}{\delta\phi^*_{imt}} - i\frac{\phi_{imt+\Delta t} - \phi_{imt-\Delta t}}{2\Delta t} = 0$$

$$\phi_{imt+\Delta t} = \phi_{imt-\Delta t} - i2\Delta t\frac{\delta\mathcal{E}}{\delta\phi^*_{imt}}$$

$$\frac{\delta\mathcal{E}}{\delta\phi^*_{imt}} \equiv H_{KS}(t)\,\phi_{imt}$$

Stability analysis: equation is time-translation invariant, thus we can consider solutions of the form

$$\phi_{imt} = f_{im}\,e^{-i\omega t}$$

Replace H_{KS} by its highest eigenvalue $\|h\|$, $\lambda = \Delta t\|h\|$

Then $\sin\omega\Delta t = \lambda \leq 1$ require $\Delta t < \frac{1}{\|h\|}$

2. FKW algorithm

$$\phi(t+\Delta t) := \sum_{n=0}^{4} \frac{(i\Delta t\, H_{KS})^n}{n!}\phi(t)$$

$\lambda = \Delta t \|h\|$ is worst case

$$e_4^{-i\Delta t\|h\|} = 1 + i\lambda - \frac{\lambda^2}{2} - i\frac{\lambda^3}{6} + \frac{\lambda^4}{24}$$

$$\text{norm } \left| e_4^{-i\Delta t\|h\|} \right|^2 = 1 - \frac{\lambda^6}{72} + \frac{\lambda^8}{576}$$

$$\leq 1 \text{ for } \lambda < \sqrt{8}$$

norm conservation for C_{60}.

$\Delta t = 0.001\ eV^{-1}$ $\quad \|h\| = 500\ eV$

consider a state at $50\ eV = E$

$$\left| e_4^{-i\Delta t E} \right|^2 = 1 - \frac{(0.05)^6}{72} = 1 - 2\times 10^{-10}$$

$$\left| e_4^{-i\Delta t E} \right|^{2\times 40{,}000} = 1 - 10^{-7}$$

In practice, energy conservation tracks with norm conservation.

3. Crank-Nicolson

$$\frac{1 - iH_{KS}\Delta t/2}{1 + iH_{KS}\Delta t/2}$$

- no norm restriction
- requires inverting a matrix

Example of C_{60}

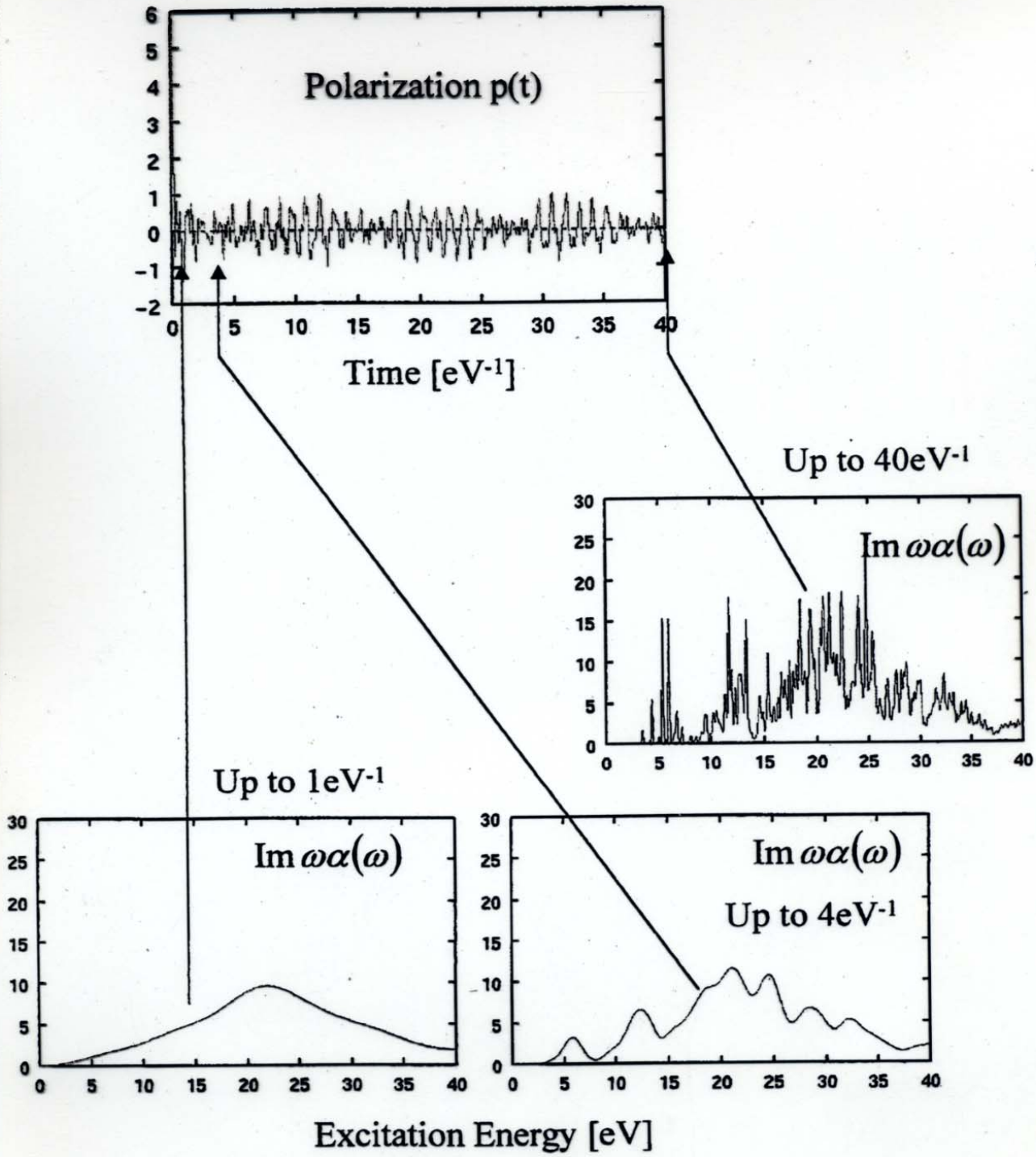

Computational Cost: C_{60} as example

Basic Operation: $\psi_i(\vec{r}, t+\Delta t) \approx \sum_{k=0}^{4} \frac{1}{k!}\left[\frac{\Delta t}{i\hbar} h\right]^k \psi_i(\vec{r}, t)$

Spatial Grid Points: N_r

Mesh spacing $h = 0.3\,\text{Å}$ $\quad \varepsilon_{\max} \approx \frac{\hbar^2}{2m}\left(\frac{\pi}{h}\right)^2 \approx 30\text{Ry}$

Occupied orbital energy $\approx$ 0.1eV accuracy

Number of mesh points $N_r \approx 64{,}000$

Points inside 7.5 Å sphere

Number of Electrons: N_e $\quad N_e = 240$

(Number of Occupied Orbitals $N_e/2$)

Time Step: $\left|h\frac{\Delta t}{\hbar}\right| \le \varepsilon_{\max}\frac{\Delta t}{\hbar} \approx 1$ $\quad \frac{\Delta t}{\hbar} = 0.001\text{eV}^{-1}$

Number of Time Steps: M_t $\quad M_t = 40{,}000$

Resolution of Spectrum $\Delta E = 2\pi\left(\frac{T}{\hbar}\right)^{-1} \approx 0.15\text{eV}$

Hamiltonian, Number of non-zero elements: $M_h \approx 100$

(Sparse matrix in mesh representation)

Storage requirement: $N_r \times N_e$ 120MB

CPU time (FP Operation): $N_r \times N_e \times M_t \times M_h \times 10$

$\approx 3\times 10^{14}$ FPO

200hours/1CPU(Vector)

$\psi_i(\vec{r}, t)$: N_r, N_e

$h(\vec{r})\psi_i(\vec{r}, t)$

Summary of real-space real-time method

1. $O(N^2)$
2. Provides entire response in one calculation
3. Can go to strong fields
4. Computational identical H_{KS} for ground state an dynamics
5. Requires use of pseudopotentials; d-orbitals problematic.
6. M_T is a large number.

Effect of Zero-Point nuclear fluctuations

Born-Oppenheimer $\Psi_R = \phi_R \chi_R$ → nuclear only

↳ electrons at fixed R

Ground state energy surface $E_{gs}(R)$ in DFT

vertical excitation energy ω_R in TDDFT

excited energy surface $E_{ex}(R) = E_{gs}(R) + \omega(R)$

Reflection approximation

tested by E. Heller, J. Chem. Phys. 68 2066 (1978)

$$\frac{df}{dE} = f_R \left(\frac{dE_{ex}}{dR}\right)^{-1} |\chi_R|^2$$

Cases

1. Na_2 – the hydrogen molecule of DFT
2. Benzene – forbidden transitions
3. Ethylene – nonharmonic in torsional mode.

Spectrum of Na_2

- vibrational fine structure.

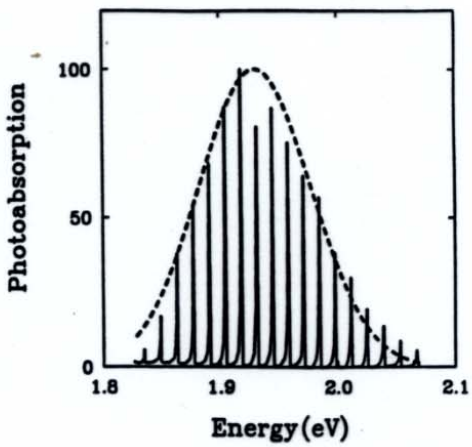

A. Herrmann, et al., Chem. Phys. Lett. (1977) 418.

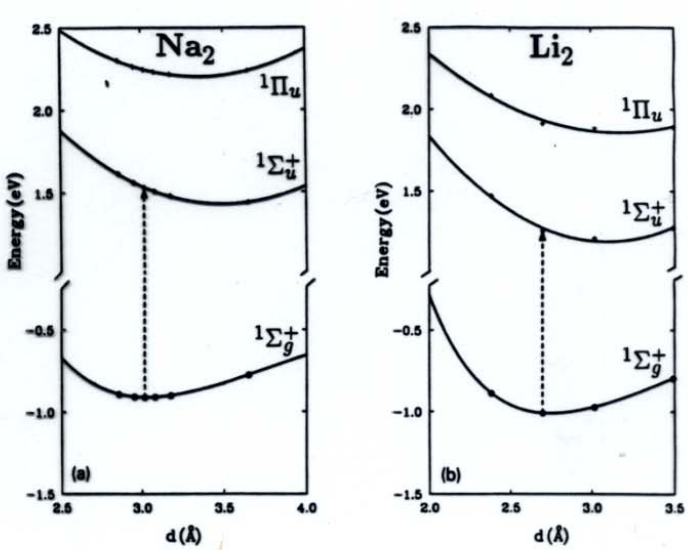

PPLDA + RPA theory:

Y. Wang, et al., Zeit. Phys. D25 (1993) 181.

Physicist's view of benzene excitations

in $\pi\pi^*$ manifold.

$$\psi_m = \sum_{k=0}^{5} e^{im\varphi_k} \psi_k$$

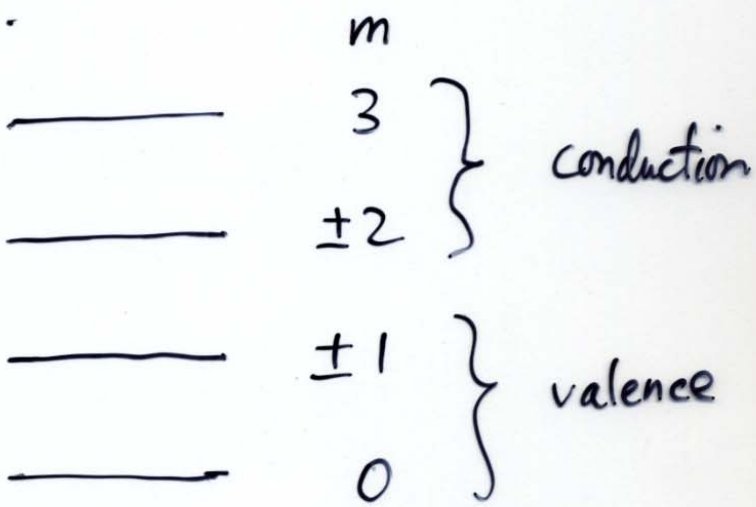

Possible transitions:

m_v	m_c	$\lvert\Delta m\rvert$	
+1	+2	1	allowed
−1	−2	1	
+1	−2	3	forbidden
−1	+2	3	

FIGURES

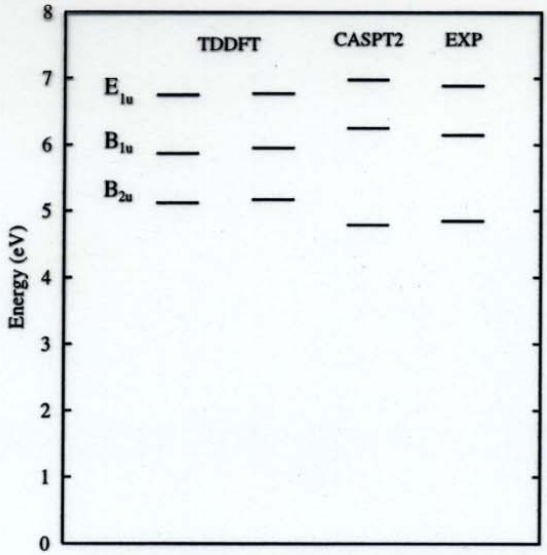

FIG. 1. Electronic excitations in benzene. The two TDDFT calculations our own (leftmost) and one of those of ref. [3] (next on right). The next level scheme shows the CI calculation of ref. [17]. The rightmost column shows the empirical spectrum as compiled in ref. [3].

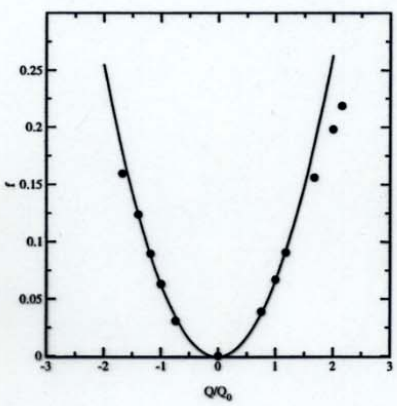

FIG. 2. Dependence of the oscillator strength of the $^1B_{1u} \leftarrow ^1 A_{1g}$ transition on the vibrational coordinate for the 8a mode, and parabolic fit.

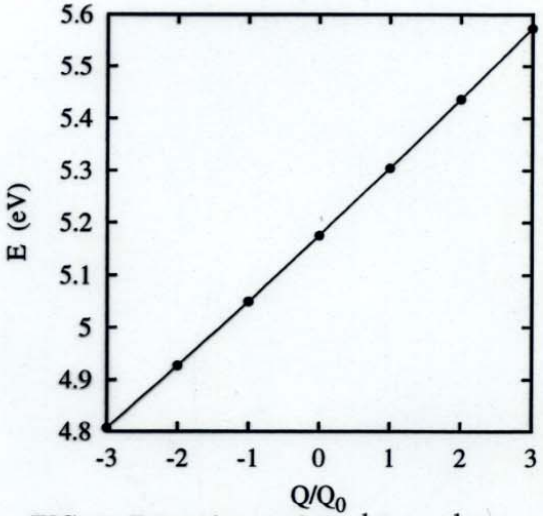

FIG. 3. Dependence of the $^1B_{2u} \leftarrow ^1 A_{1g}$ transition energy on the vibrational coordinate for the mode 1, and linear fit.

Benzene spectrum, $\pi-\pi^*$ transitions

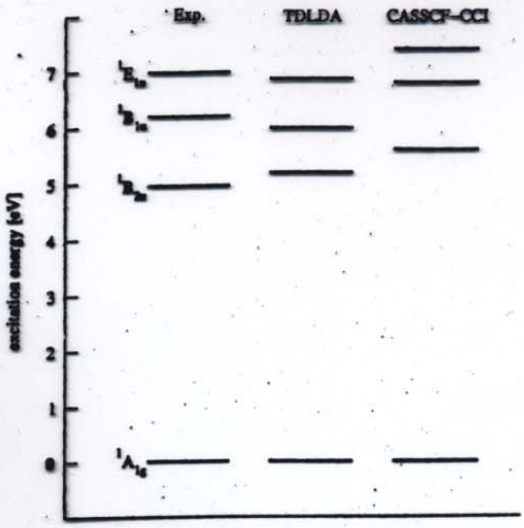

Figure 1: Singlet $\pi-\pi^*$ vertical excitation energies of benzene. Besides the experimental data the predictions of TDLDA and CASSCF-CCI [16] are given.

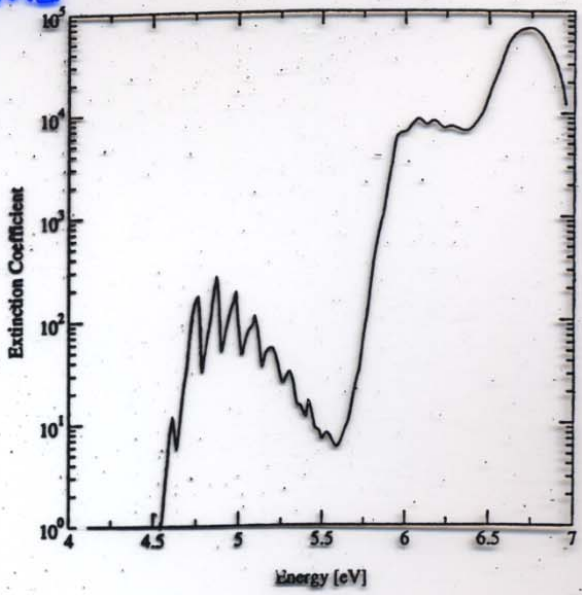

Figure 2: Low-resolution absorption spectrum of benzene in hexane solvent [4].

Electron-vibration coupling in TDDFT:
Bertsch, Schnell, Yabana, J. Chem. Phys. 115 ('01)

$f/10^{-3}$	TDDFT	CASSCF	Exp.
$^1B_{2u}$	1.6	0.5	1.3
$^1B_{1u}$	59	75	90
$^1E_{1u}$	1100		900-950

} 3 orders of magnitude!

Width	A_{1g} vibrations			CASSCF	Exp.
K_k (ev)	1	2	Tot.		
$^1B_{2u}$	0.12	0.03	0.15	0.14	0.18
$^1B_{1u}$	0.12	0.03	0.15	0.14	0.17
$^1E_{1u}$	0.12	0.03	0.15		0.125